ACS chemical biology

Articles

Cite This: ACS Chem. Biol. 2018, 13, 2498−2507

pubs.acs.org/acschemicalbiology

Mycobacterial MenJ: An Oxidoreductase Involved in Menaquinone Biosynthesis

Ashutosh Upadhyay,[†,⊥] Santosh Kumar,[†,⊥] Steven A. Rooker,[†] Jordan T. Koehn,[‡] Debbie C. Crans,[‡] Michael R. McNeil,[†] J. Shaun Lott,[§] and Dean C. Crick*[,†]

[†]Mycobacteria Research Laboratories, Department of Microbiology, Immunology and Pathology, Colorado State University, Fort Collins, Colorado 80523, United States

[‡]Chemistry Department, Colorado State University, Fort Collins, Colorado 80523, United States

[§]Biological Sciences, The University of Auckland, Auckland 1010, New Zealand

Supporting Information

ABSTRACT: MenJ, annotated as an oxidoreductase, was recently demonstrated to catalyze the reduction (saturation) of a single double bond in the isoprenyl side-chain of mycobacterial menaquinone. This modification was shown to be essential for bacterial survival in J774A.1 macrophage-like cells, suggesting that MenJ may be a conditional drug target in *Mycobacterium tuberculosis* and other pathogenic mycobacteria. Recombinant protein was expressed in a heterologous host, and the activity was characterized. Although highly regiospecific *in vivo*, the activity is not absolutely regiospecific *in vitro*; in addition, the enzyme is not specific for naphthoquinones vs benzoquinones. Coenzyme Q-1 (a benzoquinone, UQ-1) was used as the lipoquinone substrate, and NADH oxidation was followed spectrophotometrically as the activity readout. NADPH could not be substituted for NADH in the reaction mixture. The enzyme contains a FAD binding site that was 72% occupied in the purified recombinant protein. Enzyme activity was maximal at 37 °C and pH 7.0; addition of divalent cations, EDTA, and reducing agents such as dithiothreitol to the reaction mixture had no effect on activity. The addition of detergents did not stimulate activity, and addition of saturating levels of FAD had relatively little effect on the observed kinetic parameters. These properties allowed the development of a facile assay needed to study this potential drug target, which is also amenable to high throughput screening. The K_m values for UQ-1 using recombinant MenJ from *Mycobacterium smegmatis* or *M. tuberculosis* without saturating concentrations of FAD were found to be 52 ± 9.6 and 44 ± 4.8 μM, respectively, while the K_m^{NADH} values were determined to be 59 ± 14 and 64 ± 15 μM. The K_m for MK-1, the menaquinone analogue of UQ-1, using recombinant MenJ from *M. tuberculosis* without saturating concentrations of FAD but in the presence of 0.5% Tween 80 was shown to be 30 ± 2.9 μM. Thus, this is the first report of a kinetic characterization of a member of the geranylgeranyl reductase family of enzymes.

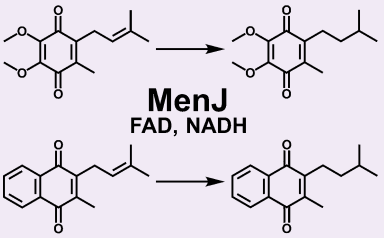

Lipoquinones play key roles in the respiratory electron transport systems (ETS) of both prokaryotes and eukaryotes by shuttling electrons between the membrane-bound electron donors (hydrogenases, dehydrogenases, and oxidoreductases) and acceptors (terminal oxidases in aerobic respiration and terminal reductases in anaerobic respiration).[1,2] These lipids can be divided into two major structural groups: ubiquinones (or benzoquinones, UQ) and menaquinones (or naphthoquinones, MK).[3] UQ and MK are characterized by the presence of an isoprenyl side-chain of varying length and degree of saturation (reduction or hydrogenation of double bonds). The variations in the structures of the lipoquinones have been used to assist taxonomic differentiation of prokaryotes for many decades,[3,4] suggesting conservation of function. Generally Gram-negative bacteria contain UQ, MK, demethylmenaquinone (DMK), or a combination; while strictly aerobic Gram-negative chemotrophs synthesize only UQ, the Gram-positive taxa synthesize MK or DMK.[3] The Gram-negative facultative anaerobe *Escherichia coli*, for example, mainly utilizes UQ-8 (ubiquinone with an isoprenyl side-chain containing eight isoprene units) in its ETS under aerobic conditions but produces increased amounts of menaquinone (MK-8) under anaerobic conditions.[5] However, the Gram-positive pathogen *Mycobacterium tuberculosis* utilizes only MK in its ETS. In mycobacteria, this molecule is predominantly MK-9(II−H_2),[6−8] a molecule that has an isoprenyl side-chain of nine isoprene units with the one in the β-position hydrogenated (saturated, see Figure 1). Many studies have reported varying degrees of regiospecific saturation of the lipoquinone isoprenyl side-chain of MK and in some cases UQ. Hydrogenation of the MK side-chain is widespread in corynebacteria and mycobacteria and is not uncommon in Archaea.

Recently, an enzyme, designated MenJ (Rv0561c), was shown to catalyze the hydrogenation of a single isoprene unit in MK of *M. tuberculosis*,[9] which results in conversion of MK-9 to MK-9(II−H_2) (Figure 1) and is highly conserved

Received: May 2, 2018
Accepted: August 9, 2018
Published: August 9, 2018

DOI: 10.1021/acschembio.8b00402
ACS Chem. Biol. 2018, 13, 2498−2507

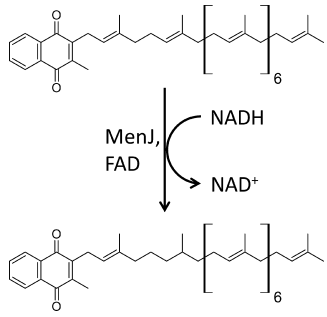

Figure 1. Reaction converting MK-9 to MK-9(II−H_2) catalyzed by $MenJ_{tb}$ (Rv0561c).

throughout both pathogenic and nonpathogenic *Mycobacterium* spp. For example, MenJ from *M. tuberculosis* ($MenJ_{tb}$) and *Mycobacterium smegmatis* ($MenJ_{smeg}$) have 74% amino acid identity with 99% coverage. Based on sequence similarity, MenJ belongs to the geranylgeranyl reductase (GGR) family of enzymes; that is, both $MenJ_{tb}$ and $MenJ_{smeg}$, to date, the only empirically identified MK saturases, were annotated as GGRs.[9] Thus, MenJ appears to represent a previously unreported subclass of GGR, which in Archaea, bacteria and plants are multifunctional enzymes that saturate multiple isoprene units of bacteriochlorophyll, chlorophyll, tocopherol, phylloquinone, and Archaeal phospholipids in a stepwise fashion.[10−12]

Data presented previously[9] indicated that the reduction of a single double bond in the isoprenoid-tail of MK by MenJ increases the efficiency of the mycobacterial ETS system. That is, MenJ deletion mutants had reduced mycobacterial electron transport efficiency, although rates of ATP synthesis and bacterial growth rates in culture were unaltered due to increased levels of total MK per bacillus.[9] Interestingly, MenJ deletion mutants grow as well as the WT bacteria in both aerobic and hypoxic conditions but have severely attenuated survival in macrophages.[9] Thus, MenJ appears to present a testable system for a contextual drug target in *M. tuberculosis*. The first steps in testing the validity of this hypothesis is development of a facile assay and characterization of the enzyme activity. Little is known about the enzymatic properties of this class of enzyme or the classical GGRs, even though crystal structures of GGRs from two of the Archaea have been determined,[13−15] presumably due to the inherent difficulties reported in assaying the activity. Using MK as a substrate in an enzyme assay presents a number of technical hurdles. MK is essentially insoluble in aqueous solutions (MK-9 has a calculated log *P* value 21.1), is sensitive to light,[16] and its absorbance and fluorescence spectra overlap those of NADH,[17,18] precluding use of a simple, sensitive spectrophotometric readout of a NADH consumption assay. Development of a facile assay required structural analysis of UQ-8 biosynthesized in *E. coli* transformed with mycobacterial *menJ* and chemical synthesis of truncated analogues of MK-9. Thus, this manuscript reports the identification of a suitable lipoquinone substrate resulting in the development of a facile, high throughput amenable *in vitro* assay for MenJ activity and the first *in vitro* characterization of the enzymatic properties of a member of the GGR family.

RESULTS AND DISCUSSION

Characterization of Lipids Extracted from *E. coli* Cells Expressing $MenJ_{smeg}$. Mycobacterial MenJ reduces a double bond in MK-8, Table 1, when expressed in *E. coli*.[9] To determine if UQ is also a substrate of $MenJ_{smeg}$, partially purified neutral lipids from control *E. coli* (transformed with empty vector) or *E. coli* transformed with *pET28a::MenJ*$_{smeg}$ were analyzed by HPLC coupled to mass spectrometry (LCMS) and tandem MS. UQ was identified by observation of protonated $[M + H]^+$ ions and verification by LC MS/MS.

Table 1. Structures and Calculated Monoisotopic Masses of Lipoquinones Described in This Study[a]

Quinones	Calculated monoisotopic masses (Da)	Structures
UQ-1	250.12051	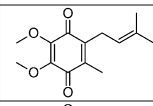
*UQ-1(H_2)	252.13616	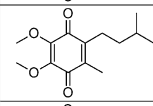
UQ-8	726.55871	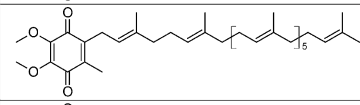
*UQ-8(H_2)	728.57436	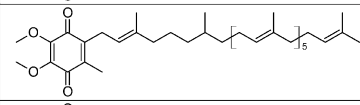
MK-1	240.11503	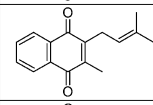
MK-4	444.30283	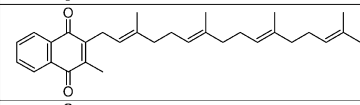
MK-8	716.55323	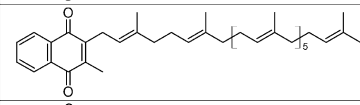
*MK-8(H_2)	718.56888	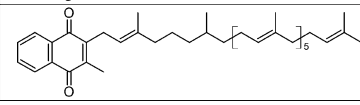

[a]Asterisks (*) indicate lipoquinones witha saturated double bond, which in UQ-8(H_2), and MK-8(H_2) is drawn to be consistent with previous reports for *M. phlei* and various other Gram-positive organisms.[6−8,21] Monoisotopic masses were calculated using ChemDraw Ultra 12.0 software (PerkinElmer Informatics).

The monoisotopic mass of UQ-8 containing 8 isoprene units, each with a single double bond, is calculated at 726.5587 Da; therefore, the expected *m/z* value for $[M + H]^+$ is 727.5667 or 729.5824 if a single double bond was reduced. Extracted ion chromatograms (EIC) were generated from total ion chromatograms (TIC) by extracting collected data for ions with $[M + H]^+$ at *m/z* 727.6 ± 0.5 or $[M + H]^+$ at *m/z* 729.6 ± 0.5 for UQ-8 and UQ-8(H_2), respectively (Figure 2). The lipids from the control strain contain a molecular feature with an observed *m/z* of 727.5611 at a retention time of 19.4 min consistent with the presence of UQ-8 but did not contain any lipids with *m/z* values that could be attributed to UQ-8(H_2) by LC-MS/MS. The observed peak at *m/z* 729.5722, coincident with *m/z* 727.5611(Figure 2A), represents an isotope peak. However, lipids extracted from *E. coli* expressing *MenJ* contained a new peak, with a retention time of about 20.2 min and an observed *m/z* value of 729.5722 in addition to the peaks at 19.4 min, indicating a gain of function consistent with the presence of UQ-8(H_2) (Figure 2B). This increase of 2 Da (727.6 to 729.6 Da) could potentially be attributed to

DOI: 10.1021/acschembio.8b00402
ACS Chem. Biol. 2018, 13, 2498−2507

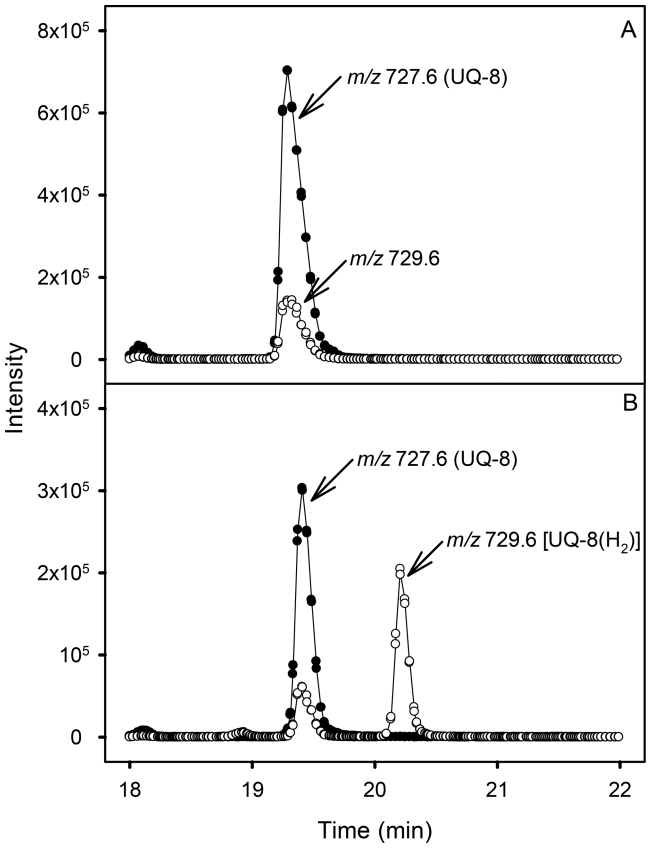

Figure 2. MenJ catalyzes the reduction of UQ-8 when expressed in *E. coli*. EIC derived from Q-TOF LC/MS analysis of partially purified lipids from recombinant *E. coli* containing pET28a empty vector (panel A) or vector containing $menJ_{smeg}$ (*MSMEG1132*) (panel B). EIC were generated from TIC by extracting data for ions with $[M + H]^+$ at m/z 727.6 ± 0.5 or m/z 729.6 ± 0.5 for UQ-8 or UQ-8(H_2), respectively.

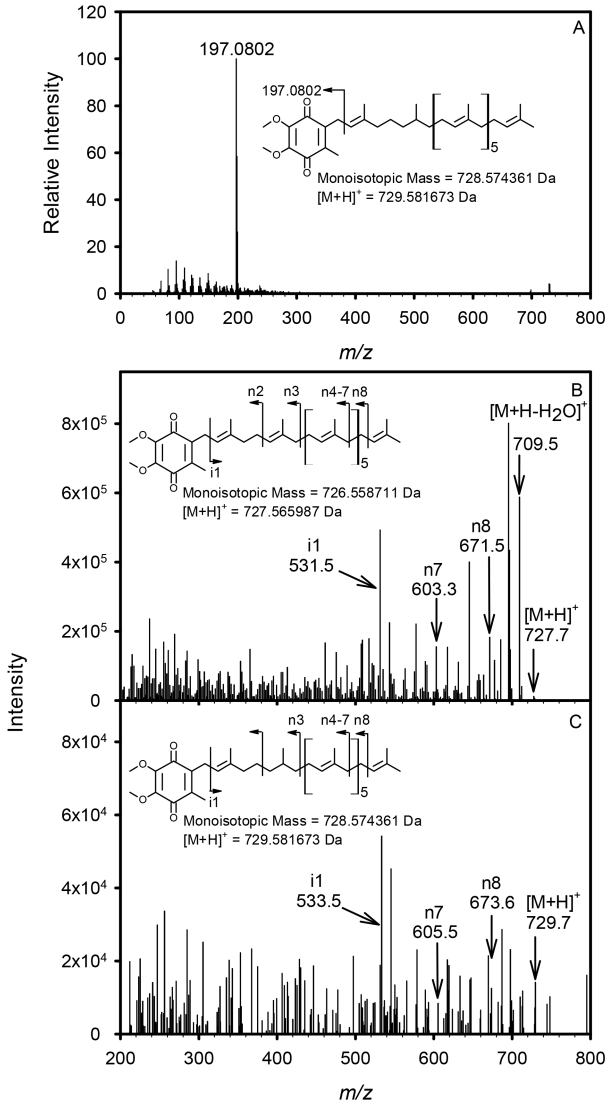

Figure 3. Tandem MS analysis of UQ-8 from recombinant *E. coli* expressing MenJ. Panel A shows a representative Q-TOF LC MS/MS analysis of ions having m/z 729.5744 identified as UQ-8(H_2) in Figure 2B, the inset shows the inferred fragmentation generating the fragment ion at m/z of 197.0802. Panels B and C show LCQ ion-trap tandem MS analysis of isoprenyl side chain of UQ-8 from WT *E. coli* and UQ-8(II−H_2) from recombinant *E. coli* expressing $MenJ_{smeg}$, respectively. The insets show the inferred fragmentation patterns.

reduction of the ketones in the benzoquinone moiety (as seen in the lipoquinone's role in electron transport), a double bond in the benzoquinone moiety, or one of the double bonds in the isoprenyl side-chain.

Tandem MS analysis of UQ molecules generate a major diagnostic fragment ion at m/z = 197.1, likely corresponding to a benzylium ion.[19,20] The molecular features with m/z values of 727.56 and 729.57, tentatively assigned as UQ-8 and UQ-8(H_2), produced major fragment ions at m/z of 197.0802 (Figure 3A) when subjected to tandem MS analysis on a Q-TOF instrument, confirming the assignment as UQ-8 and suggesting that a reduction had occurred in the isoprenoid tail and not in the aromatic ring. This conclusion was supported by LC MS/MS analysis performed on an LCQ ion-trap instrument. The resulting spectra were complex, consisting of several series of ions (Figures 3B and C). However, identification of a series of ions that retain the benzoquinone structure and differ by 68 Da (designated n2−n8) and an ion that retains only the isoprenoid moiety (designated i1) confirm the reduction in the UQ isoprenoid tail (Figure 3C). Thus, the molecular ion (m/z 729.5), $[M + H - H_2O]^+$ (m/z 711.5) and the n-series ions (m/z 605.4 and 673.5) all indicate that the molecule has a single reduced double bond near the benzoquinone ring. The fragments i1 (m/z 533.1) and n2 (calculated m/z 253.1) would identify the location of that reduction in the β-isoprene unit; however, the spectra are very complex and weak in the n2−n6 region, making unambiguous assignment of the position difficult. However, results indicate that, in addition to saturating a single double bond in the isoprenoid tail of MK as seen in mycobacteria,[9] MenJ also saturates a single double bond in the isoprenoid tail of UQ when expressed in *E. coli*. While the precise position of the saturation is difficult to identify using mass spectral methods,[6,7,9] the data point to a position close to the aromatic ring(s) in both MK and UQ. This is in agreement with earlier data that indicate that all hydrogenated MK isolated from Gram-positive eubacteria, including mycobacteria, have the β-isoprene unit from the naphthoquinone system saturated, if only one isoprene unit is saturated.[6−9,21] Thus, mycobacterial MenJ is not specific for MK vs UQ.

Expression and Purification of MenJ. The purified recombinant MenJ proteins had appropriate apparent molec-

DOI: 10.1021/acschembio.8b00402
ACS Chem. Biol. 2018, 13, 2498−2507

ular weights, and the final protein purity was consistently found to be >80−90% as judged by SDS-PAGE. The yield of the purified $MenJ_{tb}$ protein ranged from 0.7 to 1.0 mg per liter of culture.

Although $MenJ_{smeg}$ was cloned and expressed in the heterologous host *E. coli* in active form the MenJ homologue from *M. tuberculosis* is not active when expressed in *E. coli*. However, the $MenJ_{tb}$ protein complements a MenJ KO when expressed in *M. smegmatis*[9] and could be purified from this host. Although the protein is associated with membrane enriched preparations, the His tagged recombinant MenJ could be purified to at least 80% purity, as estimated by SDS-PAGE analysis, after solubilization in buffer containing an appropriate detergent. The purified recombinant protein is yellow in color in keeping with the prediction that it has a FAD binding domain [GxGxxG(x)17/18 D/E,[22] Supporting Information Figure SI1]. Bound FAD could be removed from the protein under denaturating conditions. The molar extinction coefficient of MenJ protein at 280 nm (ε_{280}) was calculated from its amino acid sequence;[23] for His_6-MenJ, ε_{280} = 72 420 M^{-1} cm^{-1},[24] and the molar extinction coefficient for FAD at 450 nm (ε_{450}) was taken to be 11 300 M^{-1} cm^{-1}. These values were used to determine the molar ratio of FAD to protein. $MenJ_{smeg}$ was found to be on average 72 ± 5% saturated with FAD when freshly purified from 3 independent preparations. Similar results were obtained for $MenJ_{tb}$. The presence of noncovalently bound FAD appears to be a characteristic of the GGR family of proteins, which has been demonstrated to be involved in electron transfer from the reducing agent to the substrate.[13] However, FAD was only associated with ∼70% of the recombinant MenJ produced in either host species.

MenJ Enzyme Activity Assay. IMAC purified MenJ was used to perform *in vitro* reductase enzyme assays. Initially, commercially available MK-4 and MK-9 (see Table 1 and Figure 1 for structures) were used as potential substrates; however, no enzyme activity could be detected. While inactivation of the enzyme during purification could not be ruled out, the insolubility of MK in aqueous solutions (MK-4 and MK-9 have calculated log *P* values of 10.9 and 21.1, respectively), its sensitivity to light[16] and absorbance/fluorescence spectra presented significant technical problems. Chemically synthesized MK-1, Scheme 1, with a calculated log *P* of 4.84, could be utilized as a lipoquinone substrate. However, this molecule required 20% Tween-80 for solubilization of the stock material in aqueous buffer and assay mixtures containing a final concentration of 0.5% of the detergent. In addition, overlap of absorption and fluorescence spectra with those of NADH required activity detection at 360 nm, a wavelength where loss of NADH absorbance could be separated from MK-1 absorbance, which is less sensitive than the more typical analysis at 340 nm (Supporting Information Figure SI2).

Because MenJ catalyzes the reduction of an appropriate isoprene unit in UQ-8, the concept of using UQ as MK analogues in *in vitro* assays was pursued. This approach has several advantages, in that UQ-1 is commercially available, of significantly greater solubility in water than available MKs, and allows for the design of a simple spectrophotometric assay. Activity detection, based on the loss of NADH absorbance at 340 nm, was utilized when UQ-1 was present in the reaction mix.

MS Analysis of *In Vitro* MenJ Assay Product. To verify that the enzyme was saturating the isoprenyl moiety rather than reducing the keto groups on the quinone core of UQ-1 *in vitro*, mass spectral analysis of the enzyme reaction product was conducted. In this case, large volume (2 mL) assays containing 1 mM UQ-1, 1.5 mM NADH, and recombinant protein (20 ng) were incubated at 37 °C for 75 min. Lipids were extracted from the reaction mixtures using chloroform/methanol (2/1) as described for the *E. coli* bacteria. After extraction of product lipids from the reaction mix, the identification of extracted lipids was carried out by LC-MS and tandem MS on the Q-TOF instrument as described above.

The monoisotopic mass of UQ-1 containing 1 isoprene unit is calculated at 250.1205 Da; therefore, the expected *m/z* value for $[M + H]^+$ is 251.1205 or 253.1441 if a double bond or the keto groups were reduced. EIC were generated from TIC by extracting collected data for ions with $[M + H]^+$ at *m/z* 251.1 ± 0.5 or $[M + H]^+$ at *m/z* 253.1 ± 0.5 for UQ-1 and UQ-1(H_2), respectively. The lipids extracted from the control assays without protein contain a molecular feature with an observed *m/z* of 251.1248 at a retention time consistent with the presence of UQ-1 but did not contain any lipids with *m/z* values that could be attributed to UQ-1(H_2) by LC-MS/MS. However, lipids extracted from assays containing MenJ contained a new peak with a retention time of about 1.2 min and an observed *m/z* value of 253.1395, indicating a gain of function consistent with the presence of UQ-1(H_2) (data not shown).

Tandem LC-MS analysis of the 251.1248 feature showed the parent ion ($[M + H]^+$), the diagnostic benzylium ion at *m/z* of 197.0802 that is presumably generated by a hydrogen transfer reaction,[19,20] and a fragment ion at *m/z* 219.1023 that is likely a vinyl carbocation generated by the loss of a methoxy group from the parent ion (Figure 4A). Tandem LC-MS analysis of the *m/z* 253.1395 peak in the product lipids also showed the molecular ion ($[M + H]^+$) and the diagnostic protonated fragment ion at *m/z* of 197.0807. However, in this case, the ion corresponding to the vinyl carbocation had an *m/z* value of 221.1167, an increase of ∼2 Da. Thus, the tandem MS analysis of the lipid extracts demonstrated that the recombinant MenJ reduced (saturated) the double bond of the isoprenoid moiety of UQ-1, and all subsequent experiments, except those to determine the K_m for MK-1, were conducted using this substrate.

Scheme 1. Synthesis of MK-1 (3)[a]

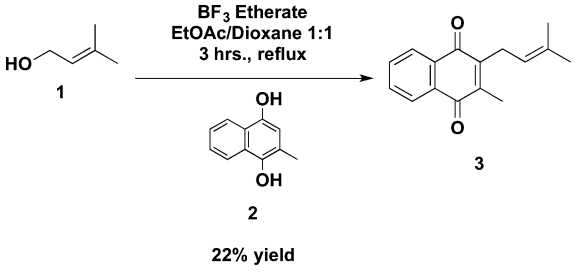

[a]MK-1, previously synthesized by other routes,[45−48] was prepared using a two-step reaction from commercially available menadione via a procedure adapted from literature.[38] Menadiol was synthesized from menadione as previously described.[36−38] Then, menadiol (**2**) was reacted with 3-methyl-2-buten-1-ol (**1**) in the presence of boron trifluoride, a Lewis acid catalyst, to attach the isoprenyl side-chain.[37,38] The coupling reaction to obtain MK-1 (**3**) resulted in a 22% yield.

DOI: 10.1021/acschembio.8b00402
ACS Chem. Biol. 2018, 13, 2498−2507

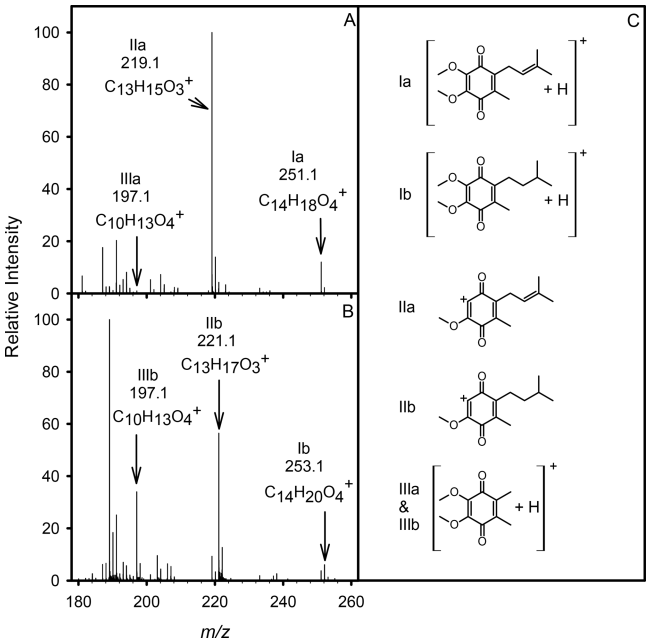

Figure 4. Tandem MS analysis of product from *in vitro* $MenJ_{smeg}$ assays showing saturation of the isoprenyl side-chain of UQ-1. A representative Q-TOF LC tandem MS analysis of MenJ reaction mix extracted with 2:1 chloroform methanol showed characteristic mass peaks for substrate UQ-1 (m/z 251.1, panel A) and product UQ-1(H_2) (m/z 253.1, panel B). The structures of diagnostic ions shown in panel C correspond to the ion peaks indicated in panels A and B. All m/z values indicated are rounded to 1 decimal place for ease of presentation, the corresponding accurate mass values are presented in the text. The 2 Da difference between ions Ia, IIa, and IIIa vs Ib, IIb, and IIIb indicates saturation of the only available isoprene unit in UQ-1.

MenJ's lack of specificity for lipoquinone (MK or UQ) allowed the development of the first facile *in vitro* assay for an enzyme of this class. Previously, kinetic analysis of GGR activity had been hampered by the requirement for complex substrates that are difficult to obtain, long incubation periods (up to 48 h), and difficult readouts based on NMR, MS, or HPLC analysis.[10,11,15,25,26]

The fact that MenJ is able to reduce the single isoprene unit available in UQ-1 indicates that although the enzyme is highly regiospecific *in vivo*[6,7] the specificity is not absolute *in vitro*. The basis of the regiospecificity of the GGR from *Sulfolobus acidocaldarius* and *Methanosarcina acetivorans*[13,27] appears to be based on accessibility of the substrate to the isoalloxazine ring of the required FAD. For example, when substrate is bound to the *S. acidocaldarius* enzyme, it can reduce three of four double bonds but not the one proximal to the phosphates in geranylgeranyl diphosphate; this appears to be because the double bond between C3 and C4 of this molecule is inaccessible to the isoalloxazine ring when the diphosphate is anchored in the anion pocket of the catalytic site.[13] However, the reduction of these double bonds is not processive, as the substrate must dissociate from the enzyme after each reduction.[15] Taken together, these observations suggest that the change from a naphthoquinone to a benzoquinone substrate may allow deeper penetration into the catalytic site of MenJ, assuming that there are geometric similarities to the GGR from *S. acidocaldarius*. However, the fact that MK-1 and UQ-1 are both substrates for the enzyme with similar kinetic constants (see below) suggests that a definitive answer as to what controls the regiospecificity of MenJ *in vivo* will require further experimentation. In that regard, determination of a crystal structure of MenJ is an ongoing a process.

Enzymatic Properties of MenJ. The activity of recombinant MenJ proteins from either source was linear with time of incubation and protein concentration for at least 30 min and up to 6 μg of protein. The enzyme activity was maximal at 37 °C and pH 7.0. Addition of supplements to the reaction mixture, including divalent cations, EDTA, and β-mercaptoethanol, had no effect on activity. The addition of CHAPS at concentrations up to 0.5% had no significant effect on the activity, but the addition of Tween 80 at 0.5% of the reaction mixture reduced the $MenJ_{smeg}$ activity by 50%. Chaps, cholate, and Tween-80 reduced the activity of $MenJ_{tb}$ by about 20%, and Triton X-100 reduced activity by 60%. It is surprising that the addition of detergents did not increase the enzyme activity. This observation is likely related to the use of UQ-1 as a substrate, as MK-1 (with a higher calculated log P) required addition of detergent for solubilization. It is likely that detergents will be required in the assay mixtures for comparison of more natural and hydrophobic (larger) benzoquinones and naphthoquinones as substrates.

Consistent with the observation that the FAD binding site was only 72% occupied in the purified recombinant protein the addition of exogenous FAD to the reaction mixture stimulated activity by approximately 30%, an effect that saturated at 10 μM with a dissociation constant of 1.3 μM.

MenJ requires two cofactors: FAD and NADH. MenJ utilizes NADH as the electron donor in catalysis, and NADPH could not be substituted as a cofactor in the reaction. This specificity seems to be unusual for a member of the GGR family. The *A. fulgidus* GGR enzyme does not appear to utilize either NADH or NADPH; the bound FAD could only be reduced using dithionite under anaerobic conditions *in vitro*.[11] Similarly, only dithionite could be used to reduce the FAD bound to the GGR from *S. acidocaldarius*;[28] however, NADH, NADPH, and dithionite were all reported to be able to sustain activity in the GGR from *T. acidophilum*.[25]

Kinetic Parameters for MenJ. The kinetic parameters for MenJ from *M. smegmatis* and *M. tuberculosis* were determined using Michaelis–Menten assumptions. The effects of UQ-1 concentration on $MenJ_{smeg}$ in the presence and absence of saturating concentrations of FAD and NADH were as shown in Figure 5. The addition of saturating levels of FAD to $MenJ_{smeg}$ had relatively little effect on the kinetic parameters associated with the UQ-1, although K_m values were unchanged, and k_{cat} values were reduced by less than 2-fold (Table 2). The $MenJ_{smeg}$ K_m values for UQ-1 as substrate without and with saturating concentrations of FAD were found to be 52 and 41 μM, respectively, at saturating concentrations of NADH. The K_m^{NADH} was determined to be 59 μM in the presence of saturating levels of UQ-1. Similar K_m values were identified for $MenJ_{tb}$, 44 and 64 μM for $K_m^{UQ\text{-}1}$ and K_m^{NADH}, respectively. The $K_m^{MK\text{-}1}$ was determined to be 30 μM for $MenJ_{tb}$ in the presence of saturating levels of NADH and 0.5% Tween-80. Surprisingly, V_{max} values for the recombinant $MenJ_{smeg}$ were 3 orders of magnitude greater than those for $MenJ_{tb}$ when normalized for protein used in the assays, and the calculated parameters k_{cat} and k_{cat}/K_m are presented in Table 2. Importantly, the affinities of $MenJ_{tb}$ for UQ-1 and MK-1 were similar at 44 and 30 μM, respectively, strengthening the

DOI: 10.1021/acschembio.8b00402
ACS Chem. Biol. 2018, 13, 2498–2507

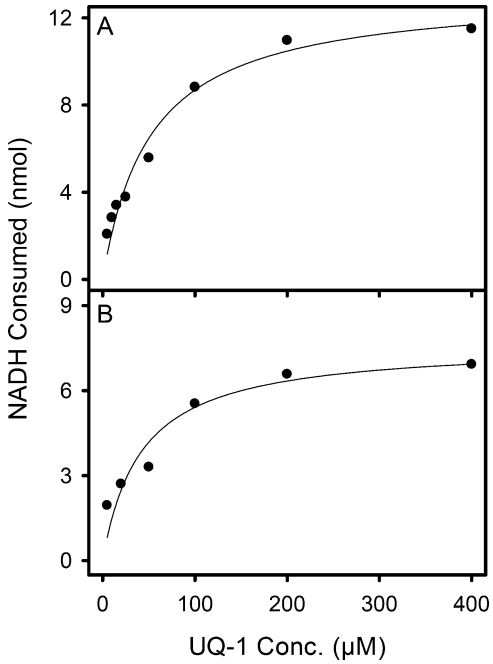

Figure 5. Representative Michaelis–Menten curves for $MenJ_{smeg}$ showing the effect of UQ-1 concentration in assays without exogenous FAD (panel A) or saturating levels (10 μM) of FAD (panel B). Assays also contained 1 ng of $MenJ_{smeg}$, 100 μM NADH, and 0.1 M McIlvaine's buffer (pH 7.0) in a final volume of 200 μL and were incubated at 37 °C for 30 min. Calculated kinetic parameters can be found in Table 2.

Table 2. Kinetic Parameters of Purified $MenJ_{tb}$ and $MenJ_{smeg}$[a]

enzyme	substrate	K_m (μM)	k_{cat} (S^{-1})	k_{cat}/K_m (S^{-1} M^{-1})
$MenJ_{tb}$	UQ-1	44 ± 4.8	0.35	7.9×10^3
	MK-1	30 ± 2.9	0.28	9.3×10^3
	NADH	64 ± 15	0.58	9.1×10^3
$MenJ_{smeg}$	UQ-1	52 ± 9.6	320	6.1×10^6
	UQ-1 + FAD	41 ± 16	180	4.5×10^6
	NADH	59 ± 14	309	5.2×10^6

[a] K_m values for UQ-1 and MK-1were determined in the presence of saturating levels of NADH and vice versa. K_m values for UQ-1 + FAD were determined in the presence of saturating levels of FAD and NADH. K_m values for MK-1 were determined in the presence of 0.5% Tween 80 and saturating levels of NADH. Assays also contained 1 ng of $MenJ_{smeg}$ or 500 ng of $MenJ_{tb}$ and 0.1 M McIlvaine's buffer (pH 7.0) in a final volume of 200 μL and were incubated at 37 °C for 30 min. The reductase activity was measured by monitoring NADH consumption spectrophotometrically by following the decrease in absorbance at 340 nm. See Figure 5 for representative concentration curves.

hypothesis that UQ-1 is an appropriate substrate for analytical purposes.

The K_m values for all of the tested substrates are approximately 2.7-fold below the reported median of 130 μM for enzymes,[29] and it is likely that the K_m for the lipoquinone will decrease as the chain length of the isoprenoid side-chain increases in size, and consequently in hydrophobicity, toward that of the natural product. The addition of saturating levels of FAD to $MenJ_{smeg}$ resulted in unchanged K_m values; however, varying the exogenous FAD concentration resulted in a saturable increase in reaction rates when both NADH and UQ-1 were at saturating concentrations. Both k_{cat} and k_{cat}/K_m values for $MenJ_{tb}$ are 3 orders of magnitude lower than those of $MenJ_{smeg}$, Table 2. Over all, k_{cat}/K_m values for $MenJ_{tb}$ are 2 orders of magnitude below the median value for all proteins,[29] while that of $MenJ_{smeg}$ is about 1.5 orders of magnitude above the median. This suggests that the selection pressure for rapid enzymatic turnover may be higher in the fast growing (3 h doubling time) *M. smegmatis* than in the slow growing (24 h doubling time) *M. tuberculosis*.[29] However, it must be remembered that the enzymes are not identical in terms of amino acid sequence and were expressed from different vectors in different heterologous hosts at different times; thus, an alternate explanation could be that the recombinant enzyme expressed in *E. coli* has a higher specific activity than that expressed in *M. smegmatis*. That is, there may be a higher proportion of active molecules in the $MenJ_{smeg}$ preparation than in the $MenJ_{tb}$ preparation, although analysis using circular dichroism did not indicate that there were significant amounts of unfolded protein in either preparation (data not shown).

Characterization of MenJ Activity from *M. smegmatis* Membranes. Having developed a reliable activity assay, reaction rates were determined in membranes isolated from *M. smegmatis*. In WT *M. smegmatis* membrane enriched preparations, NADH was oxidized independently of the addition of UQ-1 (Figure 6A). Addition of 20 μg/mL of trifluoperazine (TPZ), reported to be a specific inhibitor of mycobacterial type II NADH:menaquinone oxidoreductase,[2] abolished this activity (Figure 6A). Thus, TPZ was routinely added to assays conducted using membrane enriched fractions as the enzyme source. Introduction of UQ-1 to the assay mixture restored activity and specificity to the assay; that is, the oxidation of NADH became dependent on the addition of UQ-1. NADH oxidation was then assayed with equal amounts of protein derived from membrane preparations of WT and $MenJ_{smeg}$ KO strains of *M. smegmatis*. In the presence of TPZ and absence of UQ-1, there was no significant difference ($P \leq 0.05$, see Supporting Information) in the rates of oxidation of NADH by the two protein sources (Figure 6B and Supporting Information). When UQ-1 was added to the reaction mixture, the specific activity of the membrane fraction from the $MenJ_{smeg}$ KO was significantly ($P \leq 0.05$) less than the membrane fraction from the WT *M. smegmatis* strain a difference that can be attributed to the lack of MenJ activity in the KO strain.

Overall, results suggest that the specific activity of type II NADH:menaquinone oxidoreductase (Complex 1 of the ETS) is much greater than that of MenJ in these membrane preparations. The observed UQ-1 independent Complex 1 activity presumably utilizes endogenous MK as an electron acceptor under these conditions. Addition of UQ-1 to reaction mixtures containing TPZ restored NADH oxidation in a concentration dependent manner to membranes isolated from both WT and $\Delta MenJ_{smeg}$ strains of *M. smegmatis*, and it appears that there is little difference in the specific activity of MenJ relative to Complex 1 in membranes harvested at the mid log (OD_{600} = 0.6) or stationary (OD_{600} = 1.1) growth phase (data not shown).

CONCLUSIONS

The observations that MenJ lacks specificity for naphthoquinones over benzoquinones and does not have absolute regiospecificity *in vitro* allowed the generation of a facile

DOI: 10.1021/acschembio.8b00402
ACS Chem. Biol. 2018, 13, 2498–2507

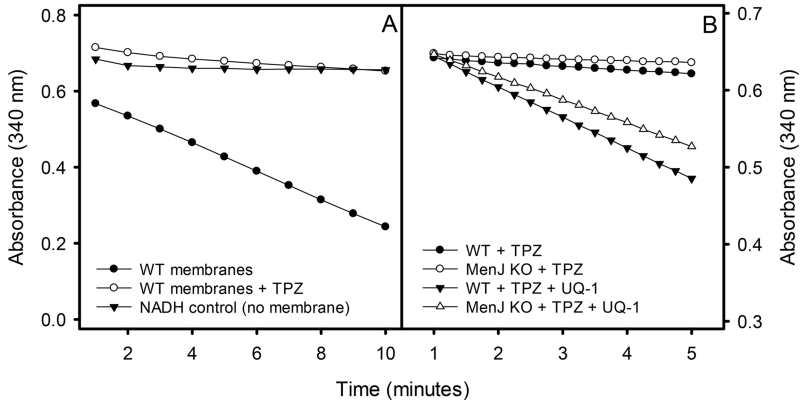

Figure 6. Effect of TPZ on oxidation of NADH by WT *M. smegmatis* membrane (panel A) and $MenJ_{smeg}$ KO membranes (panel B). Enzyme activity was measured by monitoring NADH consumption spectrophotometrically. Assays contained 15 μM NADH, 75 μM UQ-1, and 0.1 M McIlvaine's buffer (pH 7.0) in a final volume of 200 μL. TPZ was added to a final concentration of 20 μg/mL as indicated. See Supporting Information for statistical analysis.

spectrophotometry-based activity assay, more specifically, the first well characterized *in vitro* assay of a MK saturase, and the first kinetic characterization of a member of the GGR family of enzymes. The assay described herein appears to be amenable to high throughput screening (HTS) for inhibitors: it is already in 96 multiwell plate format and can easily be miniaturized to 386 well format, uses recombinant protein, is robust enough to generate reproducible data, utilizes detection of NADH consumption (which can be detected either by absorption or fluorescence changes), and is inexpensive.

MK biosynthesis in general has been proposed to be an attractive drug target in *M. tuberculosis* and potentially other Gram-positive pathogens.[30−32] Based on previous work, it is clear that MenJ is not essential for mycobacterial growth in culture.[9] However, deletion of *menJ* results in a threefold decrease in the efficiency of electron transport and severely impairs *M. tuberculosis* survival in macrophages.[9] The fact that MenJ is not an essential enzyme for bacterial growth in culture would seem to preclude its usefulness as a potential drug target. However, targeting bacterial virulence has been proposed as a paradigm for antimicrobial therapy that may circumvent, or slow, resistance mechanisms.[33−35] Usually, this would mean targeting toxin function or delivery, regulation of virulence expression, or cellular adhesion.[33] The *menJ* KO phenotype does not appear due to inhibition of toxin function or delivery, regulation of virulence expression, or cellular adhesion. It does, however, appear to fall into the proposed category of an *in vivo* essential gene target.[33] That is, MenJ activity is not essential for mycobacterial survival in culture but appears to be contextually essential for survival in host macrophages. Therefore, it is possible that MenJ represents a testable system of a contextual drug target in *M. tuberculosis*. The assay system described herein provides a necessary tool required for a search for an inhibitor of MenJ, which would not be expected to inhibit bacterial growth in culture but would inhibit bacterial growth in host cells.

METHODS

Materials and Methods. High Fidelity Taq polymerase was from Roche Diagnostics, and BCA Protein Assay Kits were purchased from Thermo Scientific Pierce. Kanamycin was from Fisher Scientific; hygromycin was from Calbiochem, and media and supplements (7H9, 7H10, OADC, LB) were from BD Difco. Vitamin K2 (MK-4), UQ-1, NADH, FAD, sodium cholate, sodium deoxycholate, goat antimouse IgG alkaline phosphatase conjugate secondary antibody, BCIP/NBT tablets, acetamide, Complete Protease Inhibitor Cocktail, Ni-NTA beads, menadione (crystalline), sodium hydrosulfite (85.0%), 1,4 dioxane (99.9%), 3-methyl-2-buten-1-ol (99%), and BF_3 etherate (≥46.5%) were purchased from Sigma-Aldrich. d_6-Dimethyl sulfoxide (99.9% + 0.05% v/v tetramethylsilane) was acquired from Cambridge Isotope Laboratories, Inc. All nonaqueous reactions were carried out under an atmosphere of argon in flame-dried glassware and were stirred on a magnetic stir plate using anhydrous solvent unless otherwise noted. All reactions in the synthesis of MK-1 were monitored by thin layer chromatography (TLC) on Whatman Partisil K6F TLC plates (silica gel 60 Å, 0.250 mm thickness) and visualized using a UV lamp (366 or 254 nm). Products were purified by flash chromatography (SiliCycle SiliaFlash F60, 43−60 μm 60 Å). Yields refer to chromatographically and spectroscopically (^{1}H NMR) homogeneous materials unless otherwise noted. Chemical shift values (δ) are reported in ppm and referenced against the internal solvent peaks in ^{1}H NMR (d_6-DMSO, δ at 2.50 ppm) and in ^{13}C NMR (d_6-DMSO, δ at 39.52 ppm). Integral values were determined using standard, uncalibrated NMR experiments and should be viewed accordingly. ^{1}H and ^{13}C spectra were recorded on a 400 MHz Varian Model MR400. NMR Spectra were processed using MestReNova version 10.0.1. High resolution mass spectrometry (HRMS) experiments for characterization of MK-1 were conducted on an Agilent 6220 TOF LC/MS ("OTOF") interfaced to an Agilent 1200 HPLC with Direct Analysis in Real Time (DART) source.

Synthesis of MK-1 [2-Methyl-3-(3-methylbut-2-en-1-yl)-naphthalene-1,4-dione]. Menadiol was synthesized from menadione as previously described,[36−38] and the procedure for the synthesis of MK-1 was adapted from previous publications for preparation of other MK derivatives.[37,38] EtOAc (8 mL) and 1,4 dioxane (8 mL) were added to a dry 50 mL round-bottom Schlenk flask, which was then purged with argon. Crude menadiol (1.50 g, 6.89 mmol, 4:1 menadiol:menadione by NMR integration) was added and stirred at 60 °C. 3-Methyl-2-buten-1-ol (0.641 g, 7.44 mmol) was added followed by dropwise addition of fresh BF_3 diethyl etherate (0.4 mL). The dark orange solution was allowed to reflux at 70 °C for 3 h under argon. The reaction was quenched with ice-water (100 mL) and extracted with diethyl ether (3 × 100 mL). The pooled organic extracts were washed with sat. $NaHCO_3$ (100 mL), followed by brine (100 mL), and dried with anhydrous Na_2SO_4. The yellow solution was then concentrated under reduced pressure at RT to yield 2.07 g of crude orange-red oil, which was subjected to flash chromatography on 230−400 mesh SiO_2 in pentane/EtOAc (20:1). MK-1, as a pure red oil, was further dried under reduced pressure overnight to yield 0.369 g (1.54 mmol) of product in 22.4% yield. ^{1}H NMR (400 MHz, d_6-DMSO) δ: 7.97−8.00 (m, 2H), 7.80−7.85 (m, 2H), 5.00 (t, J = 7 Hz, 1H), 3.29 (d, 2H, J = 7 Hz), 2.11 (s, 3H), 1.74 (s, 3H), 1.64 (s,

DOI: 10.1021/acschembio.8b00402
ACS Chem. Biol. 2018, 13, 2498−2507

3H). ^{13}C NMR (101 MHz, d_6-DMSO) δ: 184.7, 183.9, 145.1, 142.9, 133.8, 133.0, 131.55, 131.51, 125.87, 125.80, 119.4, 25.6, 25.5, 17.9, 12.4. HRMS (DART) m/z: [(M + H)$^+$] Calcd for $C_{16}H_{17}O_2$ 241.1223; Found 241.1225.

PCR Amplification, Cloning, Expression, and Purification of MenJ$_{smeg}$ and MenJ$_{tb}$. PCR amplification of *menJ$_{smeg}$* (*MSMEG1132*) was done from genomic DNA using primers with *Nde*I and *Hind*III restriction sites (underlined) engineered in the forward and reverse primers respectively; Smeg1132F ATTCATATG-AACACCCGAGCGGATGTGGTC and Smeg1132R TATAAGCTTTCAGCTGAACGGCACCCGCTG. *Taq* DNA polymerase was used for PCR amplification, and amplified gene products were cloned into the pET28a+ vector using standard molecular biology techniques.[39] The fidelity of the clone was confirmed by restriction digestion and sequencing. A confirmed clone was used to transform *E. coli* DH5α cells for expansion, purified, and used to transform *E. coli* BL21 (DE3) pLysS for expression. Recombinant protein was expressed by growing transformed bacteria in LB broth supplemented with 50 μg/mL of kanamycin at 37 °C. When the $OD_{600\ nm}$ of the culture reached 0.6, IPTG was added to a final concentration of 1.0 mM. The resulting cultures were incubated overnight; cells were harvested, washed, and disrupted by sonication in buffer A (150 mM NaCl, 1.0 mM DTT, 0.5% Triton X-100, and protease inhibitor cocktail in 50 mM phosphate buffer at pH 7.4). The homogenate was centrifuged at 15 000g for 15 min, and the supernatant was recovered. The supernatant was then incubated at 4 °C with Ni-NTA beads that had previously been equilibrated in lysis buffer. The beads were poured into a column and washed with buffer B (500 mM NaCl, 1.0 mM DTT, 0.5% Triton X-100 in 50 mM phosphate buffer, pH 7.4), and specifically bound proteins were eluted with buffer B containing 100 or 200 mM imidazol.

The *menJ$_{tb}$* (*rv0561c*) gene was PCR amplified from *M. tuberculosis* H37Rv genomic DNA using forward primer 5′-ATTCATATG-AGCGTGGATGACAGTGCCGAC-3′ and reverse primer 5′-TATAAGCTTTCAGCTGAACGGCGGTCGTCG-3′. *Nde*I and *Hind*III restriction sites are underlined. The resulting PCR products were amplified and cloned into pET28a+ vector using standard molecular biology techniques.[39] The fidelity of the clone was confirmed by restriction digestion and sequencing. Due to a lack of protein expression in *E. coli*, the Rv0561c gene was subcloned into pMyNT, an *E. coli*/mycobacteria shuttle/expression vector[40] using *Nco*I and *Hind*III restriction sites. The resulting construct was used to transform *M. smegmatis* MC^{2}155. A single, isolated colony was picked and used to inoculate 10 mL of Middlebrook 7H9 medium, supplemented with 0.2% (v/v) glycerol, 10% ADC, 0.05% Tween-80, and 50 μg/mL hygromycin, which was then incubated at 37 °C for 36 h. The resulting culture was used to inoculate 1000 mL of supplemented Middlebrook 7H9 medium and incubated at 37 °C until the OD_{600} reached 0.5−0.7. The recombinant protein expression was then induced by the addition of acetamide to a final concentration of 0.2% (w/v). The culture was then incubated for another 24−36 h at 37 °C, and cells were harvested by centrifugation, resuspended in buffer containing 50 mM Hepes and 50 mM potassium phosphate at pH 7.4, and stored at −80 °C. The frozen bacteria were thawed on ice and disrupted by sonication (described above) as needed. Sodium cholate and sodium deoxycholate (final concentration 1% each) were added to the suspension and the mixture was incubated on ice for 1 h. with gentle stirring.[41] The detergent solubilized homogenate was centrifuged at 27 000g and 4 °C for 15 min. The supernatant was then incubated with Ni-NTA beads (Sigma) at 4 °C. Bound protein was eluted with the HEPES/phosphate buffer containing imidazole.

Fractions containing the recombinant MenJ$_{smeg}$ or MenJ$_{tb}$ were identified using 12% SDS polyacrylamide gel (SDS-PAGE) visualized with Coomassie brilliant blue 250R and pooled. Imidazole was removed using PD-10 columns, and recombinant protein was concentrated as needed by ultrafiltration. The concentration of protein in the fraction of interest was determined using a BCA Protein Assay Kit with bovine serum albumin (BSA) as a standard. After resolution of proteins by SDS-PAGE, proteins were transferred to a Whatman Protran BA83 Nitrocellulose membrane using a Bis-Tris electrophoresis buffer system. The transfer blot was incubated in Tris-buffered saline pH 7.5 containing 1% BSA in for 1 h at RT. The blot was rinsed and then incubated with mouse monoclonal anti-polyHis primary antibody for 1 h. The membrane was washed three times with Tris-buffered saline pH 7.5 containing 0.1% Tween-20 at 10 min intervals. The blot was then incubated in goat antimouse IgG alkaline phosphatase conjugate secondary antibody for 1 h and developed using BCIP/NBT tablets. Recombinant protein was divided into aliquots and stored at −80 °C.

MenJ Activity Assay. For MenJ$_{smeg}$ activity assays using *M. smegmatis* membranes, cultures were harvested at the log or stationary phase of growth. Cells were washed and disrupted by sonication in buffer C (10% glycerol, 5 mM $MgCl_2$, 5 mM DTT, 50 mM phosphate buffer, pH 7.0). The homogenate was centrifuged at 27 000g for 15 min, and the supernatant was recovered. Membranes were isolated by centrifugation of the supernatant at 70 000g for 1 h, resuspended in a desired amount of buffer C, and quantified for protein content. The MenJ reaction mixtures typically contained 150 μM NADH (<1.0 $OD_{340\ nm}$), 100 μM UQ-1 as substrate and an appropriate amount of membrane protein in 0.1 M McIlvaine's buffer (pH 7.0). The reductase activity was measured by monitoring NADH consumption spectrophotometrically by following the decrease in absorbance at 340 nm in a 200 μL reaction mix at 37 °C. Complex I (NADH:menaquinone oxidoreductase) activity from the membranes was inhibited, as required, by adding 20 μg/mL of trifluoperazine (TPZ). Protein and substrate blanks were run concurrently with each assay. The decrease in absorbance due to NADH consumption was read using a BioTek Synergy HT Multi-Mode Micro Plate Reader in kinetic mode. MenJ activity assays using recombinant MenJ$_{smeg}$ or MenJ$_{tb}$, purified as described above, were performed similarly, but TPZ was omitted from the reaction mix. In cases where MK-1 was used as the lipoquinone substrate, MK-1 was solubilized in 20% Tween-80, which was diluted to a final concentration of 0.5% in the assay mixtures, and activity was monitored by change in absorbance at 360 nm (Figure SI2). All assays were conducted under conditions where the reactions were linear with regard to protein concentration and time.

Lipid Extraction and Identification. Lipid extraction from intact WT *E. coli* cells or those expressing recombinant protein was done essentially as described earlier[9,42] using chloroform/methanol (2:1, by vol.). The extracts were washed,[43] solvent was removed under a stream of N_2, lipids were dissolved in chloroform, loaded onto silicic acid columns and eluted with chloroform to effect partial purification of UQ and MK. An aliquot of the partially purified lipids was applied to a reverse-phase hypersil ODS column (Agilent) connected to an Agilent 1200 series high-performance liquid chromatography (HPLC) system. Separation was achieved using a gradient running from water to 90% methanol over 40 min at flow rate of 0.3 mL/min at 40 °C. The eluates were introduced into an Agilent 6250 quadrupole time-of-flight (Q-TOF) mass spectrometer equipped with an Agilent multimode source operated in the simultaneous electrospray ionization and atmospheric pressure chemical ionization mode (APCI). Nebulizing gas temperature was 350 °C and nebulizer pressure was 30 psi. Data obtained were analyzed using Agilent Mass Hunter Workstation software.

Samples were also analyzed using an Agilent Technologies HP1100 series HPLC connected to a Thermo 2000 Finnigan LCQ-Duo ion-trap mass spectrometer. HPLC separation was achieved using a reverse-phase XBridge C18 3.5 μm 2.1 × 150 mm column (Waters) and a gradient running from 100% methanol to methanol/isopropanol (1:1 v/v) over 50 min at 0.4 mL/min and 40 °C. Eluted molecules were subjected to positive ion MS using APCI as the ionization interface. Capillary temperature was 150 °C and APCI vaporizer temperature was 450 °C. Electrospray needle voltage was 4.5 kV. Sheath gas flow was maintained at 40 units. Data acquisition and analysis were performed using Xcaliber software from Thermo Scientific.

DOI: 10.1021/acschembio.8b00402
ACS Chem. Biol. 2018, 13, 2498−2507

In all cases, samples were spiked with known amounts of vitamin K_2 (MK-4) as an internal standard prior to extraction, and peak area[44] was used to quantitate MK.

In some cases, large scale *in vitro* assays containing 1 mM UQ-1, 1.5 mM NADH, and an appropriate amount of protein in total volumes of 2 mL were incubated at 37 °C for 75 min. Reaction products were extracted, purified, and analyzed by tandem MS using the Q-TOF mass spectrometer as described above.

Characterization of MenJ. $MenJ_{smeg}$ and $MenJ_{tb}$ are predicted to have FAD binding domains (the National Center for Biotechnology Information Web site); hence, the ratio of protein to FAD in purified recombinant MenJ was calculated. The protein concentration was first measured by UV spectroscopy followed by denaturation by heating to 100 °C for 10 min to release the bound FAD. The denatured protein was removed from solution by centrifugation at 14 500*g* for 10 min, and the FAD concentration in the supernatant was measured by spectroscopy at 450 nm. The effect of pH on MenJ activity was assayed at 37 °C and McIlvaine's buffer at various pH values under standard assay conditions. The effect of temperature was determined at pH 7 at various temperatures. To determine the effect of detergents on enzyme activity, CHAPS, Triton X-100, cholate, or Tween-80 was added to the standard reaction mix at the indicated concentrations. The effects of divalent cations, EDTA, and exogenous FAD were determined using standard assay conditions. The effect of UQ-1 concentration on MenJ activity was determined with and without exogenous FAD and in the presence of 150 μM NADH. The effect of NADH concentration on the reaction rate was determined at 200 μM UQ-1 in the reaction mix. Initial rates were used to calculate the kinetic properties of the purified enzyme, and K_m and V_{max} values were derived using Sigma Plot software (version 13).

■ ASSOCIATED CONTENT

Supporting Information

The Supporting Information is available free of charge on the ACS Publications website at DOI: 10.1021/acschembio.8b00402.

Figure SI1: Amino acid sequence alignment of the N-terminal amino acids of geranylgeranyl reductases and $MenJ_{tb}$ and $MenJ_{smeg}$; Figure SI2: UV−vis spectra of MK-1 and NADH; Figures SI3 and 4: ^1H and ^{13}C NMR spectra of MK-1; Statistical analysis of data in Figure 6B (PDF)

■ AUTHOR INFORMATION

Corresponding Author

*E-mail: Dean.Crick@colostate.edu; Tel.: (+1) 970 491 3308; Fax: (+1) 970 491 1815.

ORCID

Jordan T. Koehn: 0000-0003-3008-6303
Debbie C. Crans: 0000-0001-7792-3450
Dean C. Crick: 0000-0001-9281-7058

Author Contributions

⊥A.U. and S.K. contributed equally to this research.

Funding

Funded by NIH/NIAID Grants AI049151 and AI119567 to D.C. Crick and NSF Grant CHE-1709564 to D.C. Crans and D.C. Crick

Notes

The authors declare no competing financial interest.

■ REFERENCES

(1) Pandya, K. P., and King, H. K. (1966) Ubiquinone and menaquinone in bacteria: a comparative study of some bacterial respiratory systems. *Arch. Biochem. Biophys. 114*, 154−157.

(2) Weinstein, E. A., Yano, T., Li, L. S., Avarbock, D., Avarbock, A., Helm, D., McColm, A. A., Duncan, K., Lonsdale, J. T., and Rubin, H. (2005) Inhibitors of type II NADH:menaquinone oxidoreductase represent a class of antitubercular drugs. *Proc. Natl. Acad. Sci. U. S. A. 102*, 4548−4553.

(3) Collins, M. D., and Jones, D. (1981) Distribution of isoprenoid quinone structural types in bacteria and their taxonomic implication. *Microbiol Rev. 45*, 316−354.

(4) Jarosz, Ł., Grądzki, Z., and Kalinowski, M. (2014) Phenotypic properties and virulence factors of *Trueperella pyogenes*. *Medycna Wet 70*, 73−80.

(5) Lin, E. C., and Kuritzkes, D. R. (1987) *Pathways for Anaerobic Electron Transportin Escherichia Coli and Salmonella Typhimurium*, American Society for Microbiology, Washington DC.

(6) Azerad, R., Cyrot, M. O., and Lederer, E. (1967) Structure of the dihydromenaquinone-9 of *Mycobacterium phlei*. *Biochem. Biophys. Res. Commun. 27*, 249−252.

(7) Azerad, R., and Cyrot-Pelletier, M. O. (1973) Structure and configuration of the polyprenoid side chain of dihydromenaquinones from Myco- and Corynebacteria. *Biochimie 55*, 591−603.

(8) Dunphy, P. J., Gutnick, D. L., Phillips, P. G., and Brodie, A. F. (1968) A new natural naphthoquinone in *Mycobacterium phlei*. Cis-dihydromenaquinone-9, structure and function. *J. Biol. Chem. 243*, 398−407.

(9) Upadhyay, A., Fontes, F. L., Gonzalez-Juarrero, M., McNeil, M. R., Crans, D. C., Jackson, M., and Crick, D. C. (2015) Partial saturation of menaquinone in *Mycobacterium tuberculosis*: Function and essentiality of a novel reductase, MenJ. *ACS Cent. Sci. 1*, 292−302.

(10) Keller, Y., Bouvier, F., d'Harlingue, A., and Camara, B. (1998) Metabolic compartmentation of plastid prenyllipid biosynthesis–evidence for the involvement of a multifunctional geranylgeranyl reductase. *Eur. J. Biochem. 251*, 413−417.

(11) Hemmi, H., Takahashi, Y., Shibuya, K., Nakayama, T., and Nishino, T. (2005) Menaquinone-specific prenyl reductase from the hyperthermophilic archaeon *Archaeoglobus fulgidus*. *J. Bacteriol. 187*, 1937−1944.

(12) Addlesee, H. A., and Hunter, C. N. (2002) *Rhodospirillum rubrum* possesses a variant of the *bchP* gene, encoding geranylgeranyl-bacteriopheophytin reductase. *J. Bacteriol. 184*, 1578−1586.

(13) Sasaki, D., Fujihashi, M., Iwata, Y., Murakami, M., Yoshimura, T., Hemmi, H., and Miki, K. (2011) Structure and mutation analysis of archaeal geranylgeranyl reductase. *J. Mol. Biol. 409*, 543−557.

(14) Xu, Q., Eguchi, T., Mathews, II, Rife, C. L., Chiu, H. J., Farr, C. L., Feuerhelm, J., Jaroszewski, L., Klock, H. E., Knuth, M. W., Miller, M. D., Weekes, D., Elsliger, M. A., Deacon, A. M., Godzik, A., Lesley, S. A., and Wilson, I. A. (2010) Insights into substrate specificity of geranylgeranyl reductases revealed by the structure of digeranylgeranylglycerophospholipid reductase, an essential enzyme in the biosynthesis of archaeal membrane lipids. *J. Mol. Biol. 404*, 403−417.

(15) Kung, Y., McAndrew, R. P., Xie, X., Liu, C. C., Pereira, J. H., Adams, P. D., and Keasling, J. D. (2014) Constructing tailored isoprenoid products by structure-guided modification of geranylgeranyl reductase. *Structure 22*, 1028−1036.

(16) Dawson, R. M. C., Elliott, D.C., Elliott, W.H., and Jones, K.M. (1969) *Data for Biochemical Research*, Oxford University Press.

(17) Bondza-Kibangou, P., Millot, C., Dufer, J., and Millot, J. M. (2001) Microspectrofluorometry of autofluorescence emission from human leukemic living cells under oxidative stress. *Biol. Cell 93*, 273−280.

(18) Blacker, T. S., Mann, Z. F., Gale, J. E., Ziegler, M., Bain, A. J., Szabadkai, G., and Duchen, M. R. (2014) Separating NADH and NADPH fluorescence in live cells and tissues using FLIM. *Nat. Commun. 5*, 3936.

(19) Geyer, R., Peacock, A. D., White, D. C., Lytle, C., and Van Berkel, G. J. (2004) Atmospheric pressure chemical ionization and atmospheric pressure photoionization for simultaneous mass spectrometric analysis of microbial respiratory ubiquinones and menaquinones. *J. Mass Spectrom. 39*, 922−929.

DOI: 10.1021/acschembio.8b00402
ACS Chem. Biol. 2018, 13, 2498−2507

(20) Lytle, C. A., Gan, Y. D., Salone, K., and White, D. C. (2001) Sensitive characterization of microbial ubiquinones from biofilms by electrospray/mass spectrometry. *Environ. Microbiol. 3*, 265−272.
(21) Phillips, P. G., Dunphy, P. J., Servis, K. L., and Brodie, A. F. (1969) A new menaquinone series differing in the degree of unsaturation of the side chain. *Biochemistry 8*, 2856−2861.
(22) Dym, O., and Eisenberg, D. (2001) Sequence-structure analysis of FAD-containing proteins. *Protein Sci. 10*, 1712−1728.
(23) Pace, C. N., Vajdos, F., Fee, L., Grimsley, G., and Gray, T. (1995) How to measure and predict the molar absorption coefficient of a protein. *Protein Sci. 4*, 2411−2423.
(24) Aliverti, A., Curti, B., and Vanoni, M. A. (1999) Identifying and quantitating FAD and FMN in simple and in iron-sulfur-containing flavoproteins. *Methods Mol. Biol. 131*, 9−23.
(25) Nishimura, Y., and Eguchi, T. (2006) Biosynthesis of archaeal membrane lipids: digeranylgeranylglycerophospholipid reductase of the thermoacidophilic archaeon *Thermoplasma acidophilum*. *J. Biochem. 139*, 1073−1081.
(26) Addlesee, H. A., and Hunter, C. N. (1999) Physical mapping and functional assignment of the geranylgeranyl-bacteriochlorophyll reductase gene, *bchP*, of *Rhodobacter sphaeroides*. *J. Bacteriol. 181*, 7248−7255.
(27) Ogawa, T., Isobe, K., Mori, T., Asakawa, S., Yoshimura, T., and Hemmi, H. (2014) A novel geranylgeranyl reductase from the methanogenic archaeon *Methanosarcina acetivorans* displays unique regiospecificity. *FEBS J. 281*, 3165−3176.
(28) Sato, S., Murakami, M., Yoshimura, T., and Hemmi, H. (2008) Specific partial reduction of geranylgeranyl diphosphate by an enzyme from the thermoacidophilic archaeon *Sulfolobus acidocaldarius* yields a reactive prenyl donor, not a dead-end product. *J. Bacteriol. 190*, 3923−3929.
(29) Bar-Even, A., Noor, E., Savir, Y., Liebermeister, W., Davidi, D., Tawfik, D. S., and Milo, R. (2011) The moderately efficient enzyme: evolutionary and physicochemical trends shaping enzyme parameters. *Biochemistry 50*, 4402−4410.
(30) Lu, X., Zhou, R., Sharma, I., Li, X., Kumar, G., Swaminathan, S., Tonge, P. J., and Tan, D. S. (2012) Stable analogues of OSB-AMP: potent inhibitors of MenE, the o-succinylbenzoate-CoA synthetase from bacterial menaquinone biosynthesis. *ChemBioChem 13*, 129−136.
(31) Li, X., Liu, N., Zhang, H., Knudson, S. E., Li, H. J., Lai, C. T., Simmerling, C., Slayden, R. A., and Tonge, P. J. (2011) CoA adducts of 4-oxo-4-phenylbut-2-enoates: Inhibitors of MenB from the *Mycobacterium tuberculosis* menaquinone biosynthesis pathway. *ACS Med. Chem. Lett. 2*, 818−823.
(32) Debnath, J., Siricilla, S., Wan, B., Crick, D. C., Lenaerts, A. J., Franzblau, S. G., and Kurosu, M. (2012) Discovery of selective menaquinone biosynthesis inhibitors against *Mycobacterium tuberculosis*. *J. Med. Chem. 55*, 3739−3755.
(33) Clatworthy, A. E., Pierson, E., and Hung, D. T. (2007) Targeting virulence: a new paradigm for antimicrobial therapy. *Nat. Chem. Biol. 3*, 541−548.
(34) Allen, R. C., Popat, R., Diggle, S. P., and Brown, S. P. (2014) Targeting virulence: can we make evolution-proof drugs? *Nat. Rev. Microbiol. 12*, 300−308.
(35) Rasko, D. A., and Sperandio, V. (2010) Anti-virulence strategies to combat bacteria-mediated disease. *Nat. Rev. Drug Discovery 9*, 117−128.
(36) Payne, R. J., Daines, A. M., Clark, B. M., and Abell, A. D. (2004) Synthesis and protein conjugation studies of vitamin K analogues. *Bioorg. Med. Chem. 12*, 5785−5791.
(37) Koehn, J. T., Magallanes, E. S., Peters, B. J., Beuning, C. N., Haase, A. A., Zhu, M. J., Rithner, C. D., Crick, D. C., and Crans, D. C. (2018) A synthetic isoprenoid lipoquinone, menaquinone-2, adopts a folded conformation in solution and at a model membrane interface. *J. Org. Chem. 83*, 275−288.
(38) Suhara, Y., Wada, A., Tachibana, Y., Watanabe, M., Nakamura, K., Nakagawa, K., and Okano, T. (2010) Structure-activity relationships in the conversion of vitamin K analogues into menaquinone-4. Substrates essential to the synthesis of menaquinone-4 in cultured human cell lines. *Bioorg. Med. Chem. 18*, 3116−3124.
(39) Maniatis, T., Fritsch, E. F., and Sambrook, J. (1983) *Molecular Cloning: A Laboratory Manual*, Cold Spring Harbor Laboratory, New York.
(40) Noens, E. E., Williams, C., Anandhakrishnan, M., Poulsen, C., Ehebauer, M. T., and Wilmanns, M. (2011) Improved mycobacterial protein production using a *Mycobacterium smegmatis* groEL1DeltaC expression strain. *BMC Biotechnol. 11*, 27.
(41) Yano, T., Li, L. S., Weinstein, E., Teh, J. S., and Rubin, H. (2006) Steady-state kinetics and inhibitory action of antitubercular phenothiazines on *Mycobacterium tuberculosis* type-II NADH-menaquinone oxidoreductase (NDH-2). *J. Biol. Chem. 281*, 11456−11463.
(42) Dhiman, R. K., Mahapatra, S., Slayden, R. A., Boyne, M. E., Lenaerts, A., Hinshaw, J. C., Angala, S. K., Chatterjee, D., Biswas, K., Narayanasamy, P., Kurosu, M., and Crick, D. C. (2009) Menaquinone synthesis is critical for maintaining mycobacterial viability during exponential growth and recovery from non-replicating persistence. *Mol. Microbiol. 72*, 85−97.
(43) Folch, J., Lees, M., and Sloane Stanley, G. H. (1957) A simple method for the isolation and purification of total lipides from animal tissues. *J. Biol. Chem. 226*, 497−509.
(44) Wasinger, V. C., Zeng, M., and Yau, Y. (2013) Current status and advances in quantitative proteomic mass spectrometry. *Int. J. Proteomics 2013*, 180605.
(45) Hagiwara, E., Hatanaka, Y., Gohda, K., and Hiyama, T. (1995) Allylation of quinones with allyl(trifluoro)silanes - direct synthesis of isoprenoid quinones. *Tetrahedron Lett. 36*, 2773−2776.
(46) Mal, D., Ghosh, K., and Jana, S. (2015) Synthesis of vitamin K and related naphthoquinones via demethoxycarbonylative annulations and a retro-Wittig rearrangement. *Org. Lett. 17*, 5800−5803.
(47) Teitelbaum, A. M., Scian, M., Nelson, W. L., and Rettie, A. E. (2015) Efficient syntheses of vitamin K chain-shortened acid metabolites. *Synthesis 47*, 944−948.
(48) Yamago, S., Hashidume, M., and Yoshida, J. (2002) A new synthetic route to substituted quinones by radical-mediated coupling of organotellurium compounds with quinones. *Tetrahedron 58*, 6805−6813.

DOI: 10.1021/acschembio.8b00402
ACS Chem. Biol. 2018, 13, 2498−2507